NNLO Photon Production with Realistic Photon Isolation

Robin Schürmann

Based on 2201.06982, 2205.01516

LoopFest XX

Physik-Institut, Universität Zürich

Work in collaboration with X. Chen, T. Gehrmann, E. W. N. Glover, M. Höfer and A. Huss

Swiss National Science Foundation

Universität Zürich[UZH]

European Research Council
Established by the European Commission

Outline

1. Photons in hadronic collisions: fragmentation and isolation

2. Antenna subtraction with identified final-state particles

3. Numerical results

Photons @ the LHC

Three different kinds of photons in hadronic collisions:

1. Direct photons

→ point-like coupling of quarks and photons

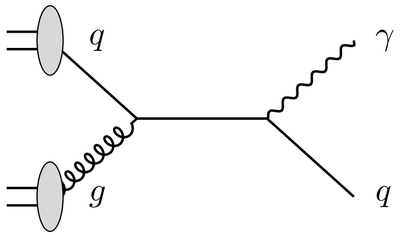

2. Partons fragmenting into photons

→ fragmentation functions (FF) $D_{k\to\gamma}(z)$

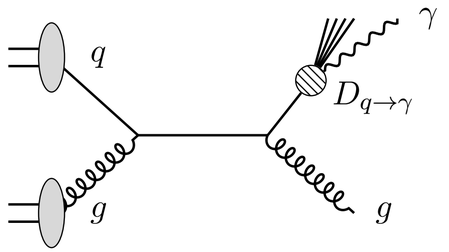

3. Photons from hadronic decays ($\pi^0 \to \gamma\gamma$)

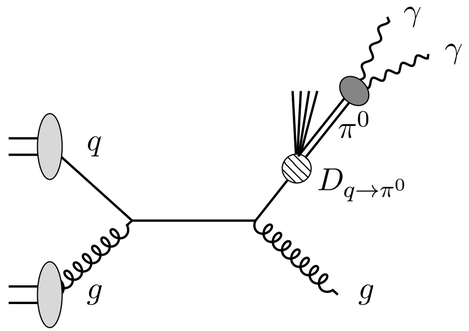

Photon Isolation

Fixed cone isolation

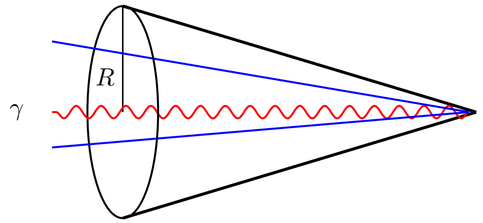

$$R^2 = \Delta\eta^2 + \Delta\phi^2$$

$$E_T^{\text{had}} < E_T^{\text{max}}(E_T^{\gamma})$$

- Used in experimental analyses
- $q \parallel \gamma$ singularity
- σ contains fragmentation contribution

Smooth cone isolation S. Frixione 1998

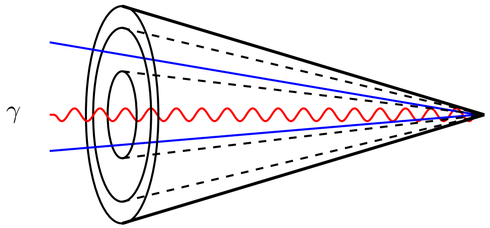

arbitrary cones with $r_d < R$

$$E_T^{\text{had}}(r_d) < \epsilon E_T^{\gamma} \left(\frac{1-\cos(r_d)}{1-\cos(R)} \right)^n$$

- Idealised photon isolation
- No $q \parallel \gamma$ singularity
- σ has no fragmentation contribution

Theory Predictions

$$\mathrm{d}\hat{\sigma}^{\gamma+X} = \mathrm{d}\hat{\sigma}^{\gamma+X}_{\mathrm{dir}} + \sum_{p} \mathrm{d}\hat{\sigma}_{p} \otimes D_{p\to\gamma}$$

Only with fixed cone isolation

NNLO QCD with idealised isolation

J. M. Campbell et al., 2017
X. Chen et al., 2019

NLO QCD with fixed cone isolation

P. Aurenche et al., 1993
S. Catani et al., 2002

New NNLO QCD calculation with fixed cone isolation

- Overcoming systematic uncertainty from mismatch of photon isolation in theory and experiment
- Implementing fragmentation processes in NNLOJET
- Extending antenna subtraction to allow for identified final-state particles

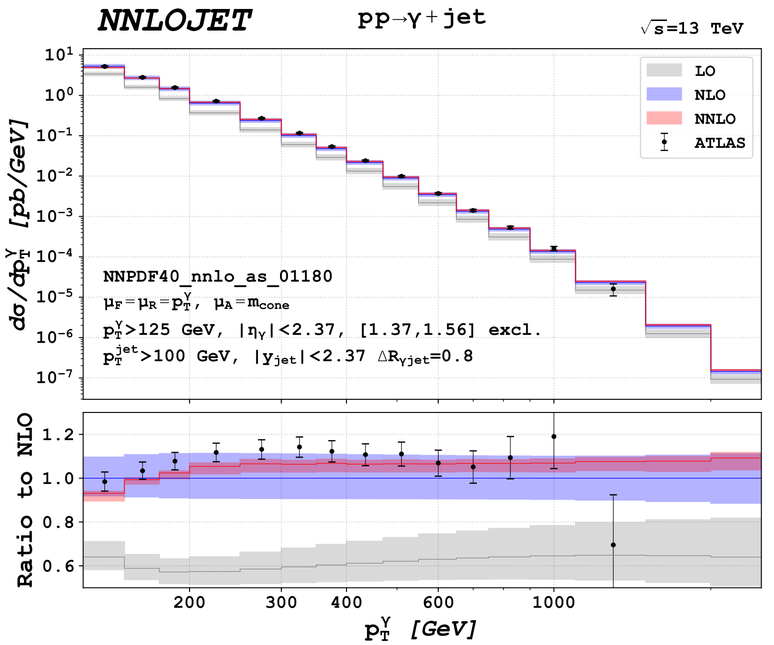

Fragmentation Antenna Functions

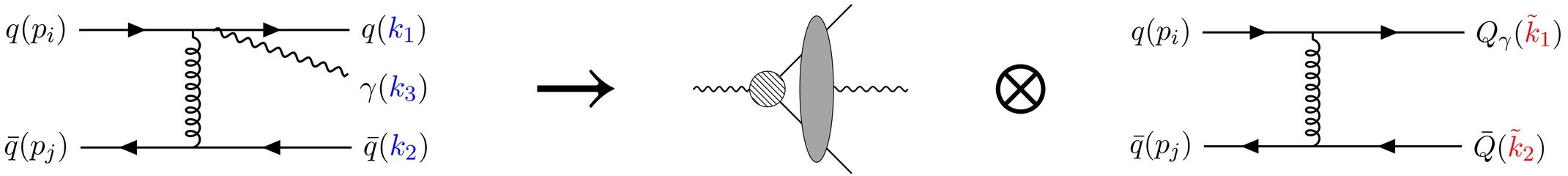

$$\mathrm{d}\sigma^S \propto A_3^0(q(k_1), \gamma^{\mathrm{id.}}(k_3), \bar{q}(k_3)) \, |M_2^0(\tilde{k}_1, \tilde{k}_2, p_i, p_j)|^2 \, J(\tilde{k}_1, \tilde{k}_2; z) \, \mathrm{d}\Phi_3$$

- Information on photon momentum in unresolved limits has to be retained

  → **extension of antenna subtraction to identified final-state particles**
- New phase space mapping and new class of antenna functions required
- Computation of final-state momentum fraction z
- **fragmentation antenna functions** $\mathcal{X}(z)$ depend on final-state momentum fraction

Numerical Results

Applications of the new NNLO calculation with realistic photon isolation

1. Precision Phenomenology

- Overcome mismatch between photon isolations in experiment and theory prediction
- Needed for comparison to data at the percent level

2. Alternative isolation parameters and isolation prescriptions

- Raise $E_T^{\max} \rightarrow$ higher sensitivity on photon fragmentation
- Democratic clustering / no photon isolation

3. Possibility to constrain the photon fragmentation functions from LHC data

- Which observables provide a high sensitivity on photon fragmentation
- New observable z_{rec}

Photon Production Cross Section

$\mathrm{d}\hat{\sigma}^{\gamma+X}$ receives contributions from direct photons and fragmentation photons:

Power Counting for fragmentation functions: $D_{q\to\gamma}(\mu_A, z) = \mathcal{O}(\alpha)$ and $D_{g\to\gamma}(\mu_A, z) = \mathcal{O}(\alpha)$

Composition of the cross section:

$$\mathrm{d}\hat{\sigma}^{\gamma+X,\mathrm{LO}} = \mathrm{d}\hat{\sigma}_{\gamma}^{\mathrm{LO}}$$

$$\mathrm{d}\hat{\sigma}^{\gamma+X,\mathrm{NLO}} = \mathrm{d}\hat{\sigma}_{\gamma}^{\mathrm{NLO}} + \mathrm{d}\hat{\sigma}_{\mathrm{MF}}^{\mathrm{NLO}} + \sum_{p} \mathrm{d}\hat{\sigma}_{p}^{\mathrm{LO}} \otimes D_{p\to\gamma}$$

$$\mathrm{d}\hat{\sigma}^{\gamma+X,\mathrm{NNLO}} = \mathrm{d}\hat{\sigma}_{\gamma}^{\mathrm{NNLO}} + \mathrm{d}\hat{\sigma}_{\mathrm{MF}}^{\mathrm{NNLO}} + \sum_{p} \mathrm{d}\hat{\sigma}_{p}^{\mathrm{NLO}} \otimes D_{p\to\gamma}$$

Choice of fragmentation scale μ_A:

- Without isolation: $\mu_A = p_T^{\gamma}$
- In presence of isolation: $\mu_A = m_{\mathrm{cone}}$
  with $m_{\mathrm{cone}}^2 = E_T^{\mathrm{max}} p_T^{\gamma} R^2 + \mathcal{O}(R^4)$
  $\mu_F = \mu_R = p_T^{\gamma} \gg \mu_A$

Choice of fragmentation functions:
BFG2 set L. Bourhis et al., 1998

Numerical Results

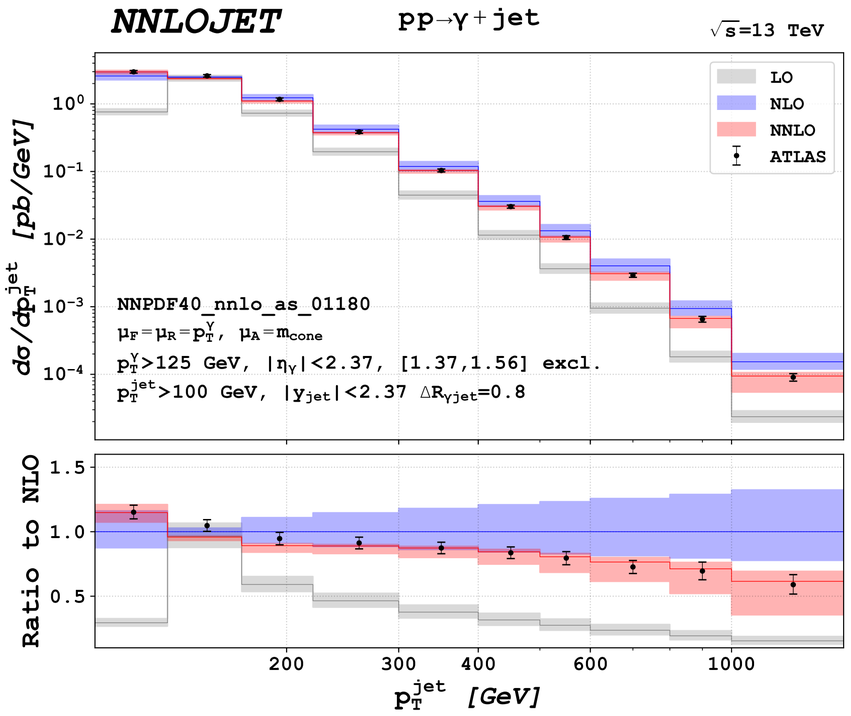

ATLAS 13 TeV γ + jet study (ATLAS, 2018):

Fixed cone isolation:

$R = 0.4, E_T^{\max} = 0.0042\, p_T^{\gamma} + 10\,\mathrm{GeV}$

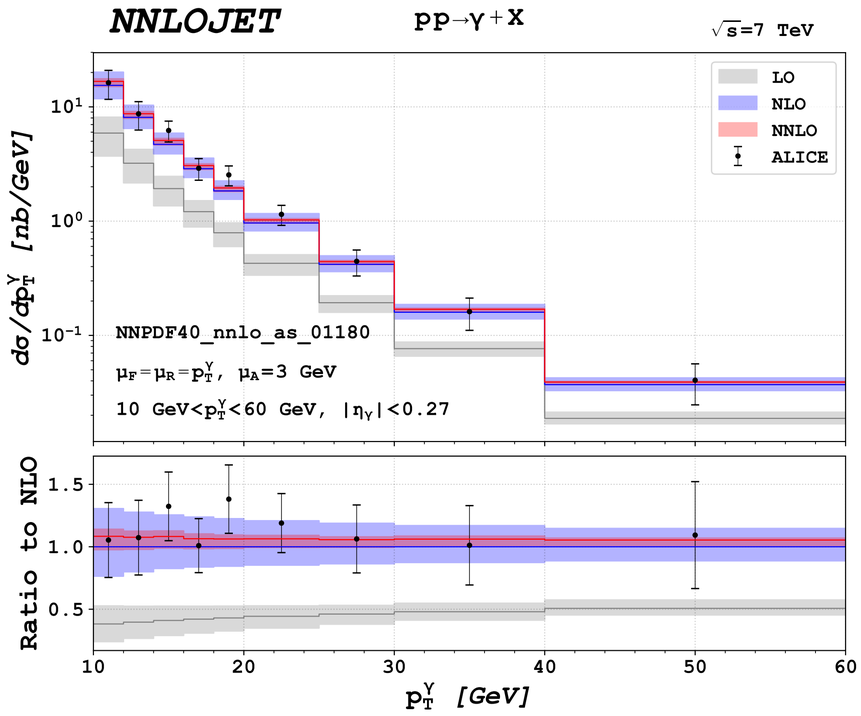

ALICE 7 TeV isolated photon study (ALICE, 2019):

Fixed cone isolation:

$R = 0.4, E_T^{\max} = 2\,\mathrm{GeV}$

Numerical Results: $\mathrm{d}\sigma/\mathrm{d}p_T^\gamma$

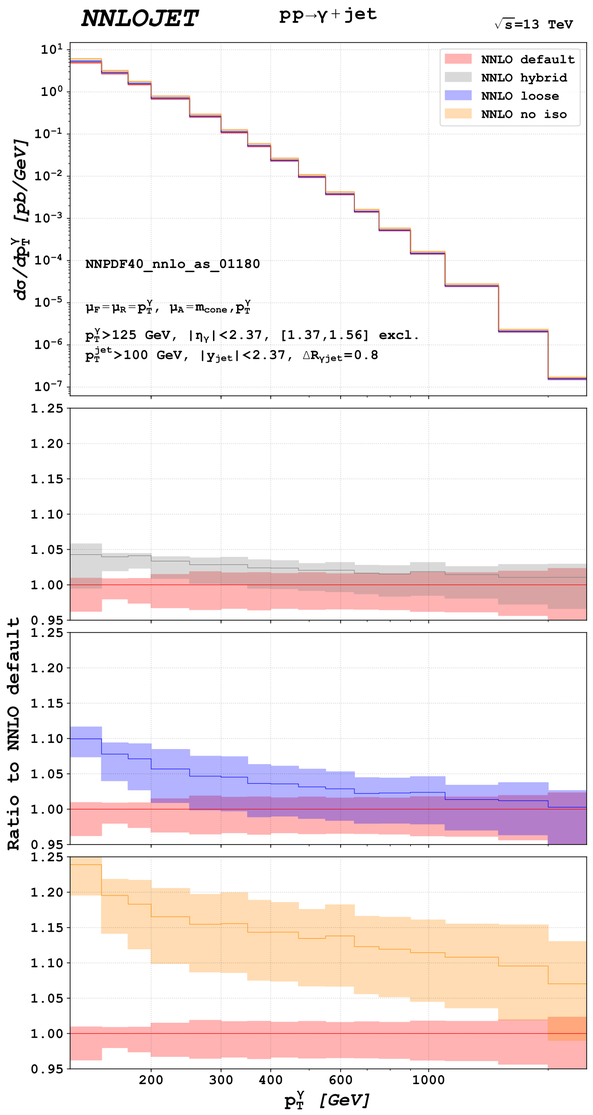

Comparison of different isolations:

- Cone based isolations ($R = 0.4$):
  - Default isolation: $E_T^{\max} \approx 10\,\mathrm{GeV}$
  - Hybrid isolation: default isolation + smooth cone ($R_{\mathrm{inner}} = 0.1$)
  - Loose isolation: $E_T^{\max} \approx 50\,\mathrm{GeV}$
- Non-isolated cross section

Photon transverse momentum distribution:

- Cone-based isolations deviate at small transverse momenta
- At large p_T^γ: photon well separated from hadronic energy

Numerical Results: $\mathrm{d}\sigma/\mathrm{d}p_T^{\gamma}$

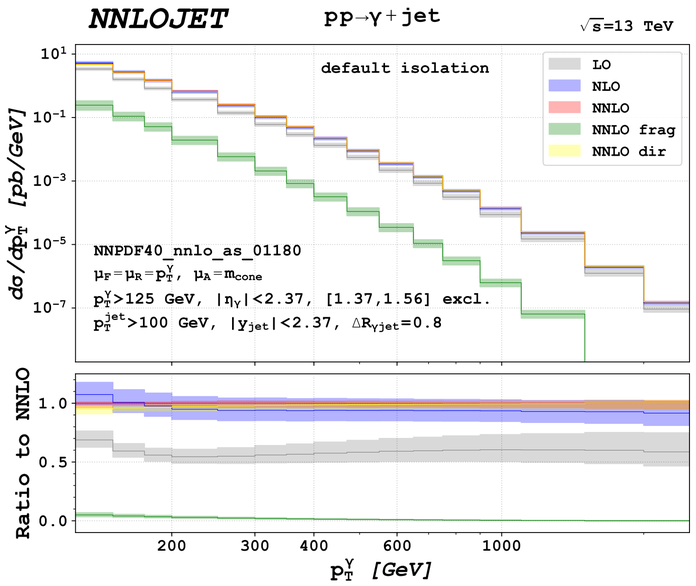

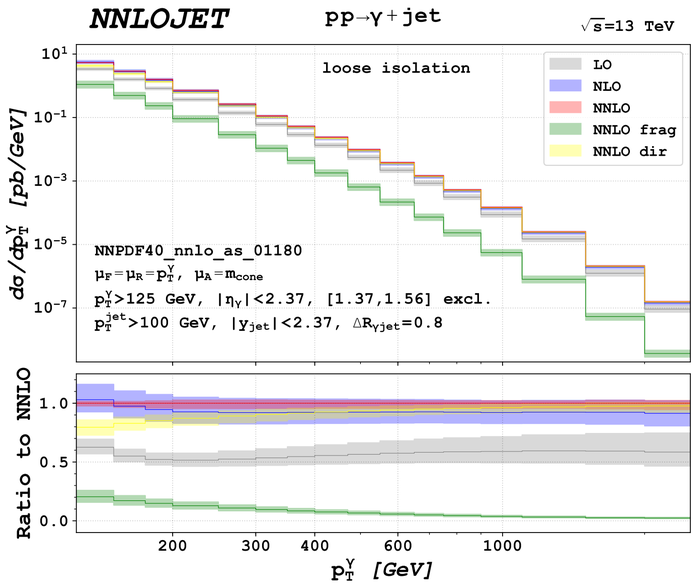

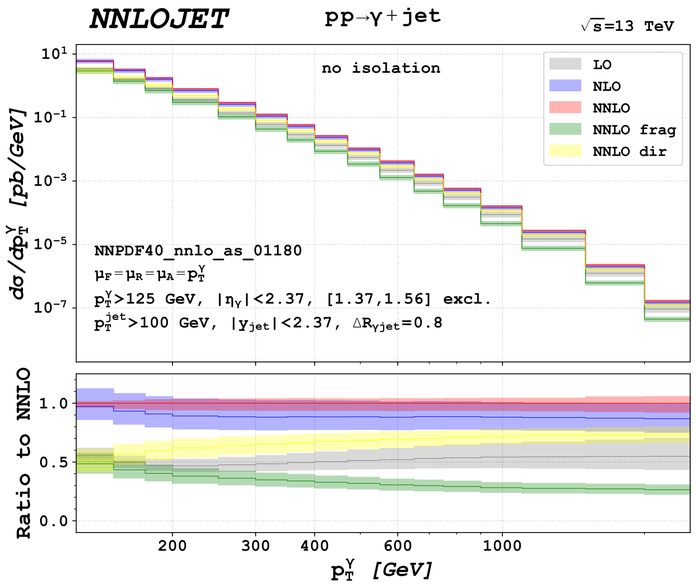

<u>Photon transverse momentum distribution:</u>

- Largest sensitivity on fragmentation processes at low p_T^{γ}
- For tightly isolated photon production: small fragmentation contribution
- Fragmentation increases with increasing $E_T^{\max}$

Numerical Results: $\mathrm{d}\sigma/\mathrm{d}p_T^{\mathrm{jet}}$

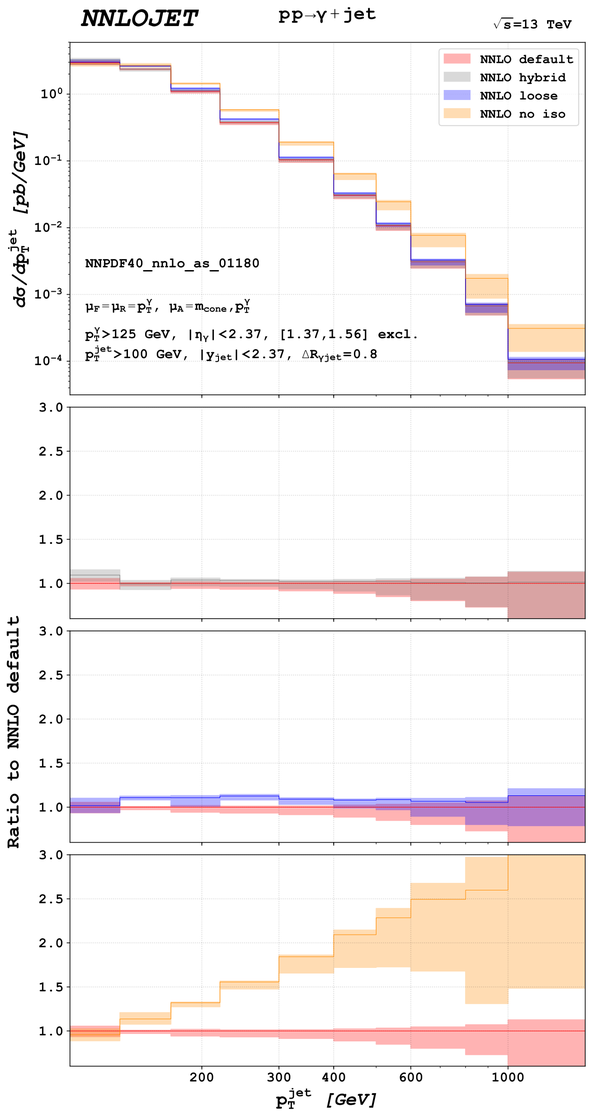

Comparison of different isolations:

- Cone based isolations ($R = 0.4$):
  - Default isolation: $E_T^{\max} \approx 10\,\mathrm{GeV}$
  - Hybrid isolation: default isolation + smooth cone ($R_{\mathrm{inner}} = 0.1$)
  - Loose isolation: $E_T^{\max} \approx 50\,\mathrm{GeV}$
- Non-isolated cross section

Jet transverse momentum distribution:

- Cone-based isolations deviate at small and mid transverse momenta
- Strong enhancement of the non-isolated cross section at high p_T^{jet}

  →fragmentation photons accompanied by hadronic energy

Numerical Results: $\mathrm{d}\sigma/\mathrm{d}p_T^{\mathrm{jet}}$

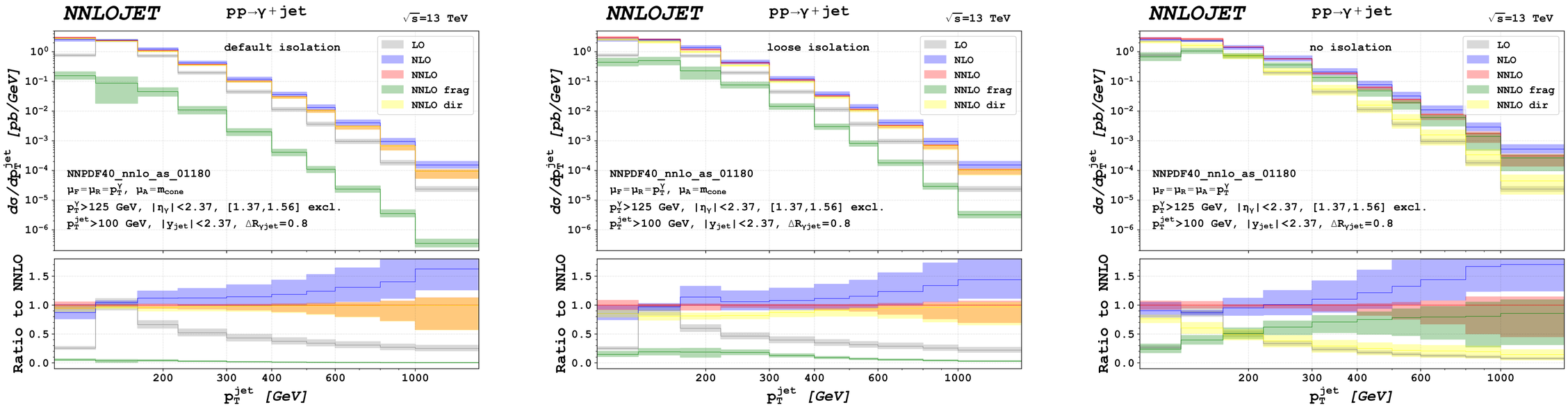

Jet transverse momentum distribution:

- Isolated photon production: largest sensitivity on fragmentation processes at low p_T^{jet}
- Non-isolated photon production: high-p_T^{jet} regime dominated by fragmentation photons
- Fragmentation increases with increasing E_T^{max}

New Observable: z_{rec}

Imbalance of photon and jet transverse momenta: $z_{\mathrm{rec}} = \dfrac{p_T^{\gamma}}{p_T^{\mathrm{jet}}}$

→yields differential sensitivity on the photon fragmentation functions

Leading order for direct photons:

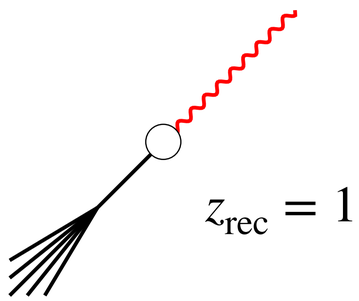

Lowest order for fragmentation photons:

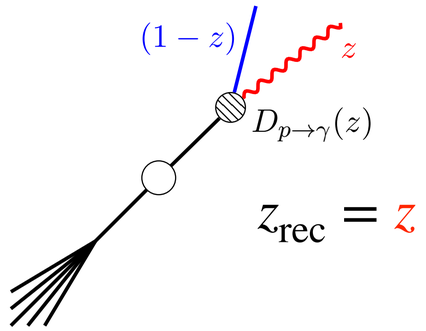

($z_{\mathrm{rec}} = z$ does not hold beyond lowest order)

New Observable: z_{rec}

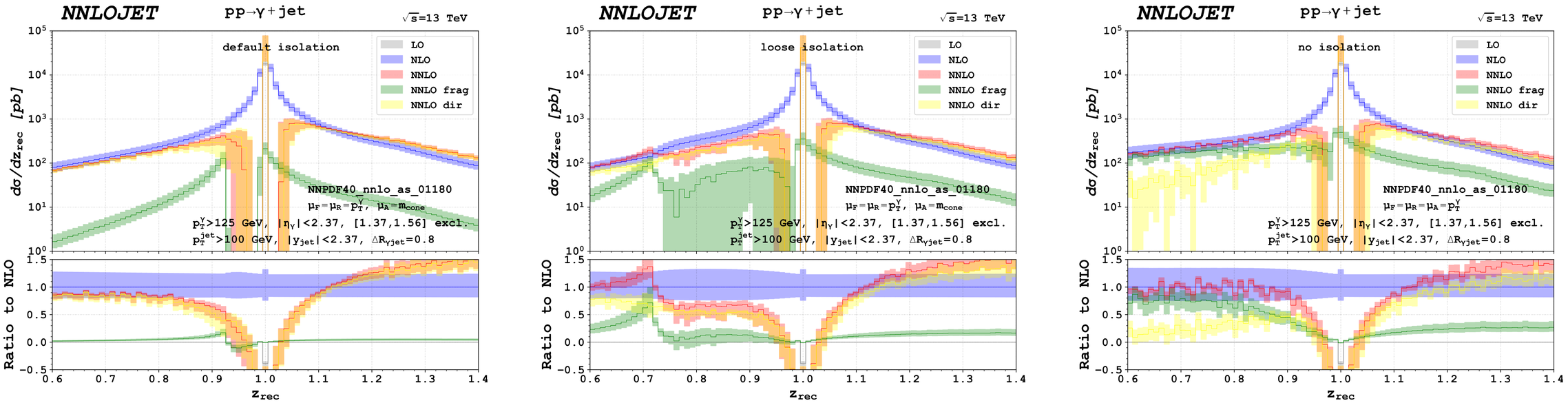

z_{rec}-distribution:

- Sudakov shoulder at $z_{\mathrm{rec}} = 1 \rightarrow$ resummation needed for reliable results in this regime
- Isolated photon production: instability at $z_{\mathrm{rec}} = z_{\mathrm{rec}}^{\mathrm{min}} \rightarrow$ minimal momentum fraction for fragmentation photons at lowest order
- Non-isolated photon production: fragmentation processes dominate for $z_{\mathrm{rec}} < 1$

Conclusion

- First NNLO calculation of the photon production cross section with realistic photon isolation (crucial for comparison to data at this level of precision)

- Requires identification of final-state photons in unresolved limits

- Strongest sensitivity on photon isolation and photon fragmentation in the low p_T^{γ}- and low p_T^{jet}-region

- Possibility to constrain the photon fragmentation functions with LHC data
  - Looser isolations needed (ideally no isolation at all!)
  - Differential sensitivity through z_{rec}

Thank you for your attention!

BACKUP

Numerical Results

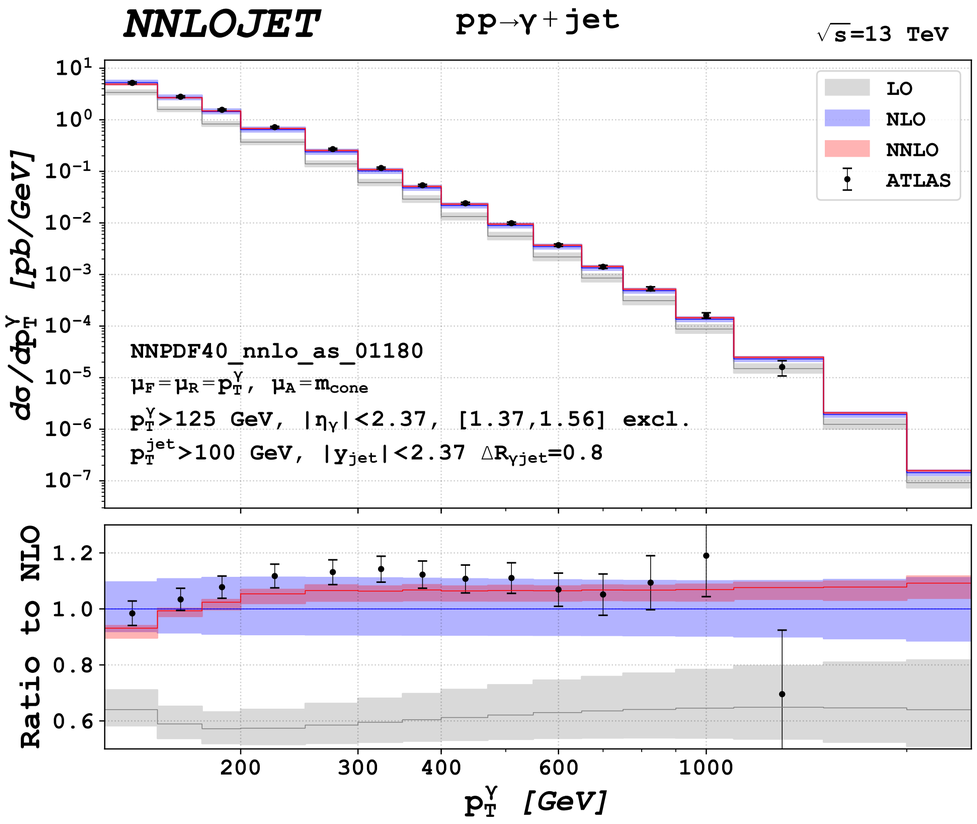

ATLAS 13 TeV γ + jet study (ATLAS, 2018):

$p_T^\gamma > 125\,\text{GeV}, |y_\gamma| < 2.37$ excl. [1.37,1.56]

$p_T^{\text{jet}} > 100\,\text{GeV}, |y_{\text{jet}}| < 2.37$

Fixed cone isolation: $R = 0.4$, $E_T^{\text{max}} = 0.0042\,p_T^\gamma + 10\,\text{GeV}$

Numerical Results

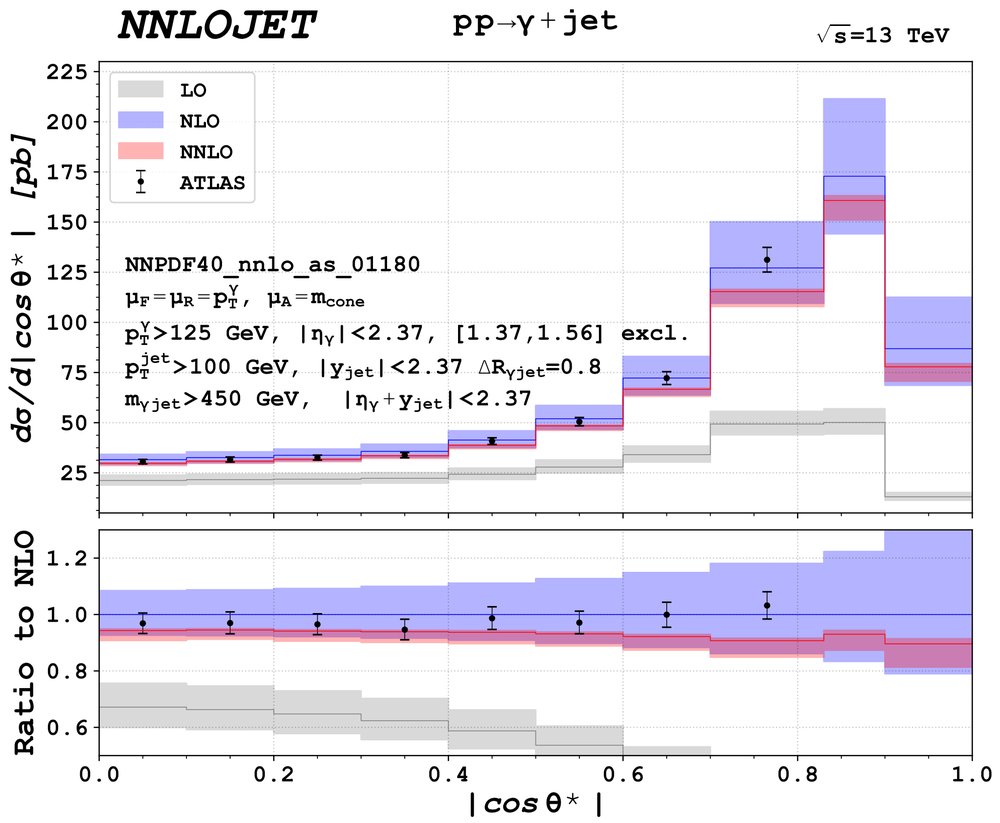

ATLAS 13 TeV γ + jet study (ATLAS, 2018):

$p_T^\gamma > 125\,\text{GeV}, |y_\gamma| < 2.37$ excl. [1.37,1.56]

$p_T^{\text{jet}} > 100\,\text{GeV}, |y_{\text{jet}}| < 2.37$

Fixed cone isolation: $R = 0.4$, $E_T^{\text{max}} = 0.0042\,p_T^\gamma + 10\,\text{GeV}$

Numerical Results

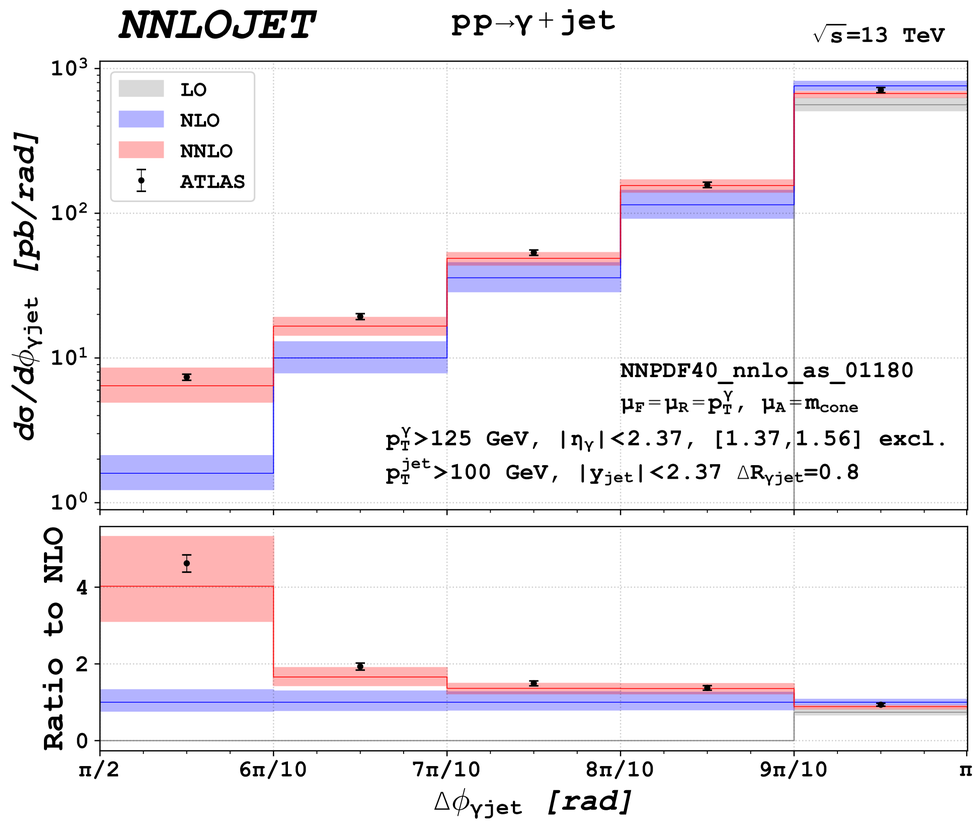

ATLAS 13 TeV γ + jet study (ATLAS, 2018):

$p_T^\gamma > 125\,\text{GeV}, |y_\gamma| < 2.37$ excl. [1.37,1.56]

$p_T^{\text{jet}} > 100\,\text{GeV}, |y_{\text{jet}}| < 2.37$

Fixed cone isolation: $R = 0.4$, $E_T^{\text{max}} = 0.0042\,p_T^\gamma + 10\,\text{GeV}$

Numerical Results

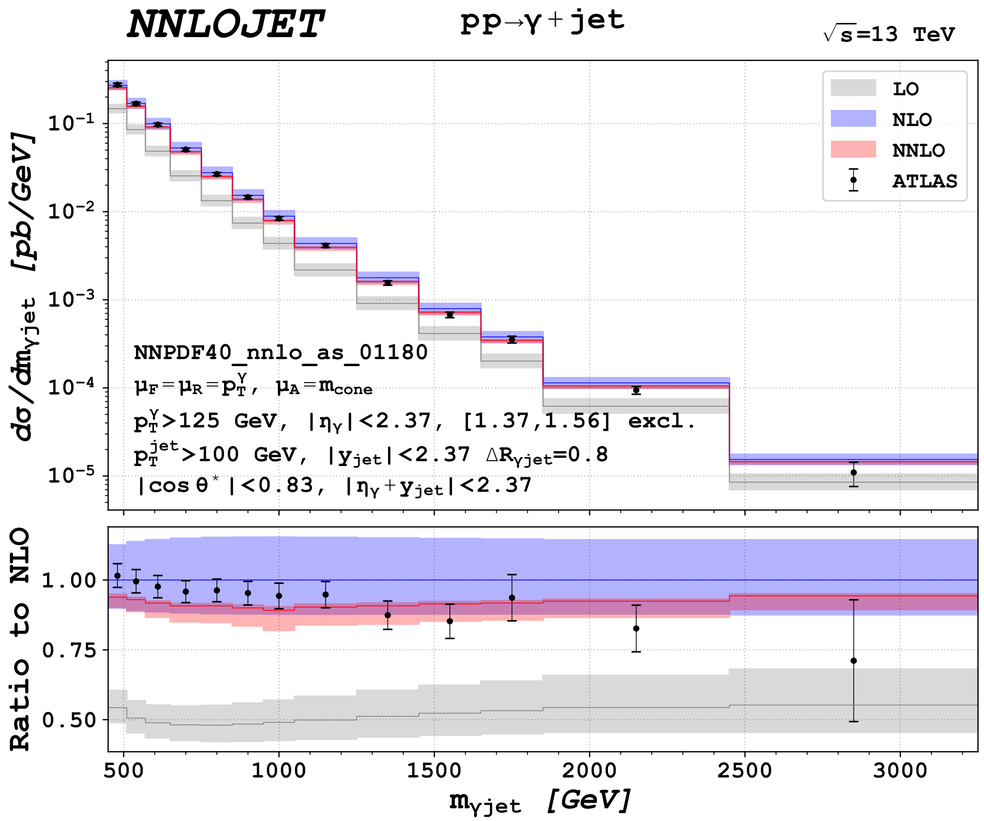

ATLAS 13 TeV γ + jet study (ATLAS, 2018):

$p_T^\gamma > 125\,\text{GeV}, |y_\gamma| < 2.37$ excl. [1.37,1.56]

$p_T^{\text{jet}} > 100\,\text{GeV}, |y_{\text{jet}}| < 2.37$

Fixed cone isolation: $R = 0.4$, $E_T^{\text{max}} = 0.0042\,p_T^\gamma + 10\,\text{GeV}$

Numerical Results: $\mathrm{d}\sigma/\mathrm{d}\,|\cos\theta^*|$

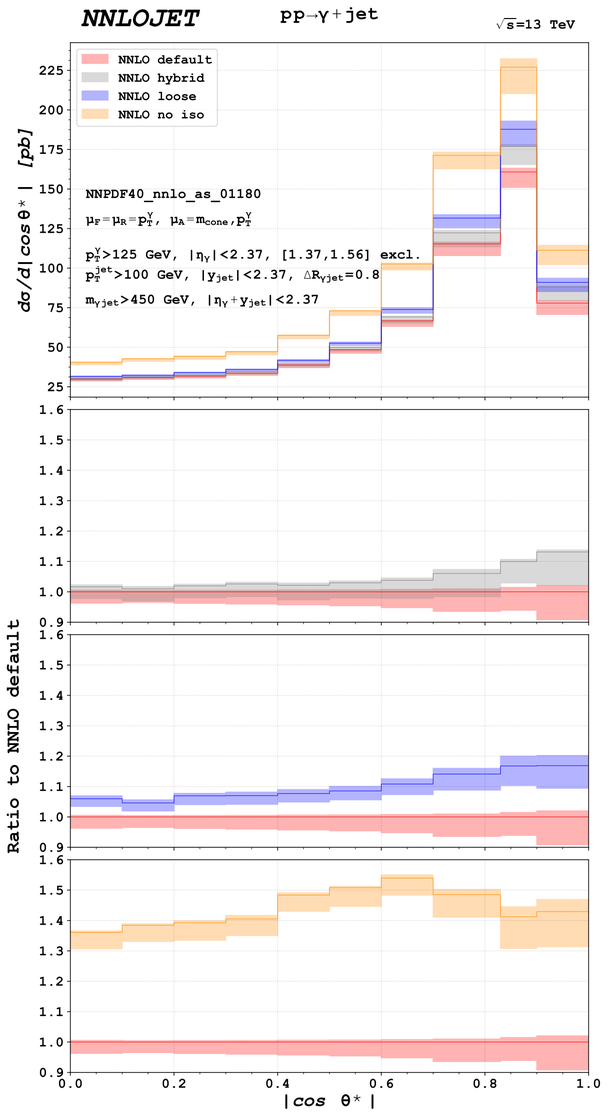

Comparison of different isolations:

- Cone based isolations ($R = 0.4$):
  - Default isolation: $E_T^{\max} \approx 10\,\mathrm{GeV}$
  - Hybrid isolation: default isolation + smooth cone ($R_{\mathrm{inner}} = 0.1$)
  - Loose isolation: $E_T^{\max} \approx 50\,\mathrm{GeV}$
- Non-isolated cross section

$\cos\theta^*$-distribution:

- $\cos\theta^* \equiv \tanh(\Delta y/2)$

  $\rightarrow \theta^*$ polar scattering angle of the underlying $2 \rightarrow 2$ scattering event
- Largest sensitivity on photon isolation in high $\cos\theta^*$-region

Numerical Results: $\mathrm{d}\sigma/\mathrm{d}\,|\cos\theta^*|$

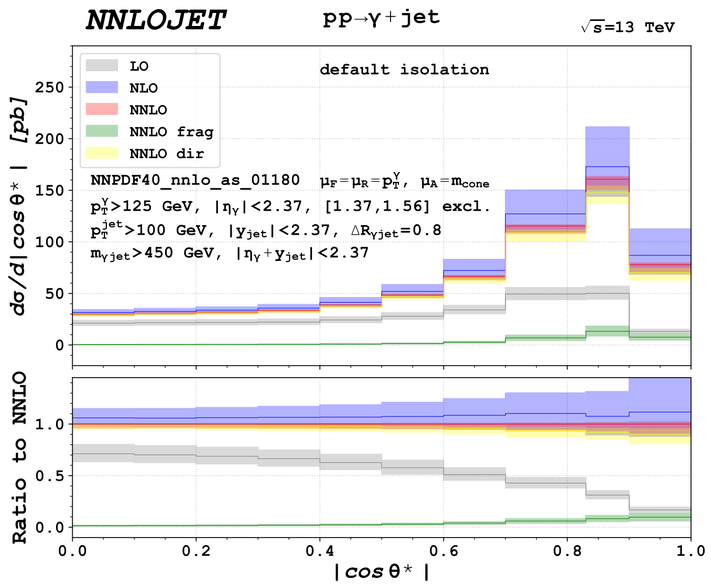

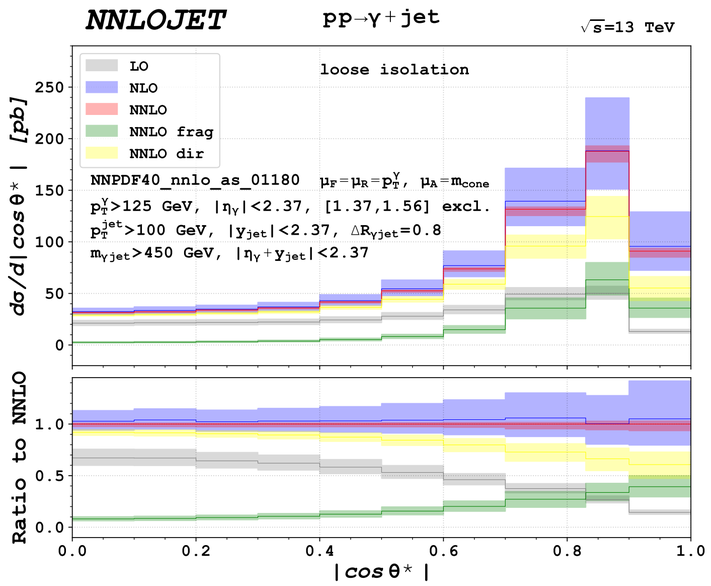

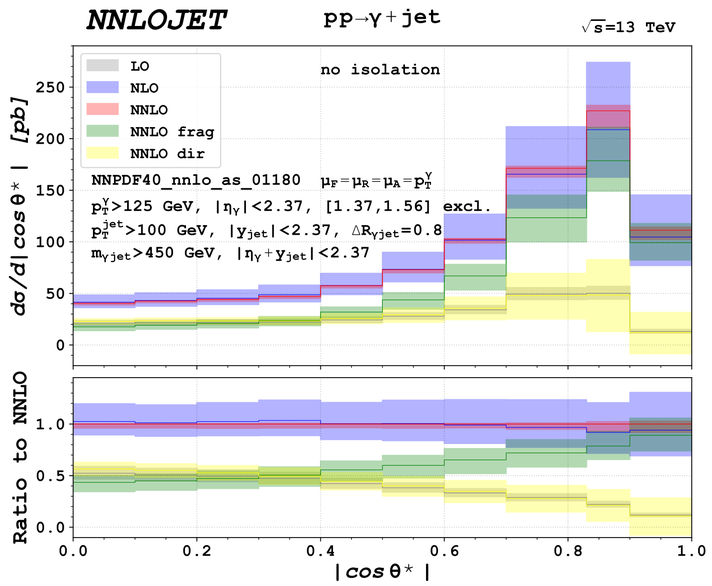

<u>$\cos\theta^*$-distribution:</u>

- θ^* polar scattering angle of the underlying $2 \to 2$ scattering event: $\cos\theta^* \equiv \tanh(\Delta y/2)$
- Different dependence on $|\cos\theta^*|$ for direct and fragmentation contribution → fragmentation contribution increases towards larger $|\cos\theta^*|$
- Fragmentation increases with increasing $E_T^{\max}$

Antenna Subtraction

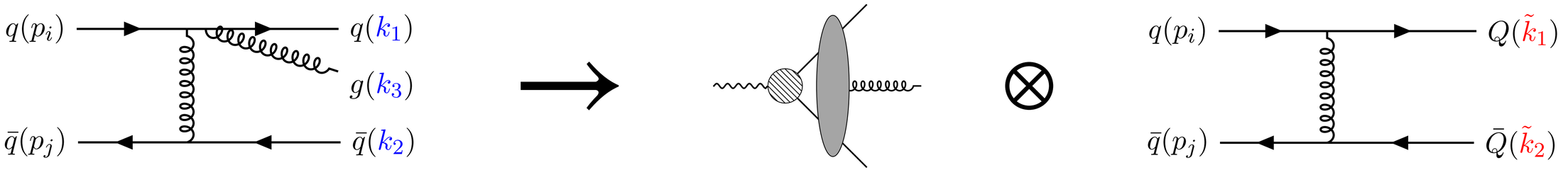

$$\mathrm{d}\sigma^S \propto A_3^0(q(k_1), g(k_3), \bar{q}(k_3)) \, |M_2^0(\tilde{k}_1, \tilde{k}_2, p_i, p_j)|^2 \, J(\tilde{k}_1, \tilde{k}_2) \, \mathrm{d}\Phi_3$$

- Only dependence on $\{k_1, k_2, k_3\}$ in antenna function
- Jet function and reduced matrix element only depend on mapped momenta $\{\tilde{k}_1, \tilde{k}_2\}$

→ phase space can be factorised

$$\mathrm{d}\sigma^T \propto \underbrace{\left(\int \mathrm{d}\Phi_A A_3^0(q(k_1), g(k_2), \bar{q}(k_3)) \right)}_{\mathscr{A}_3^0} |M_2^0(\tilde{k}_1, \tilde{k}_2; p_i, p_j)|^2 \, J(\tilde{k}_1, \tilde{k}_2) \, \mathrm{d}\Phi_2$$

→ explicit ϵ-poles in $\mathscr{A}_3^0$

Fragmentation Antenna Functions

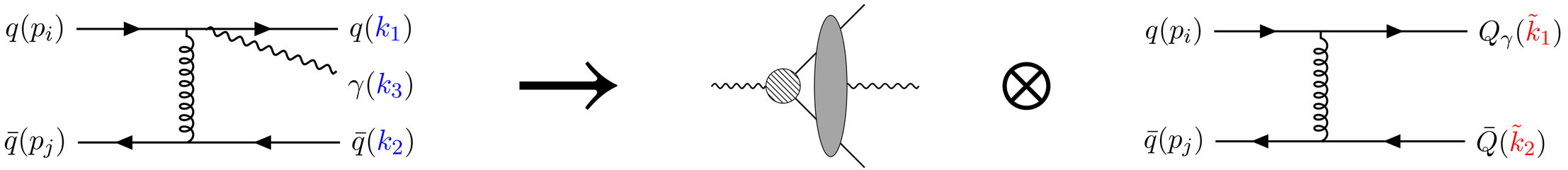

$$\mathrm{d}\sigma^S \propto A_3^0(q(k_1), \gamma^{\mathrm{id.}}(k_3), \bar{q}(k_3)) \, |M_2^0(\tilde{k}_1, \tilde{k}_2, p_i, p_j)|^2 \, J(\tilde{k}_1, \tilde{k}_2; z) \, \mathrm{d}\Phi_3$$

Jet function needs information about momentum fraction z of the photon within the quark-photon cluster Q_γ:

$$z = \frac{s_{23}}{s_{23} + s_{12}} \overset{q \parallel \gamma}{\to} \frac{E_\gamma}{E_\gamma + E_q}$$

Reconstruction of photon and quark momentum in photon isolation and jet algorithm:

$$\tilde{k}_1 \to \{z\,\tilde{k}_1, (1-z)\,\tilde{k}_1\}$$

Fragmentation Antenna Functions

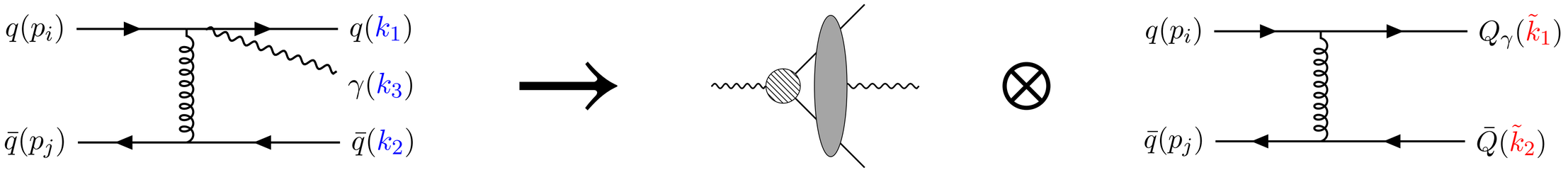

$$\mathrm{d}\sigma^S \propto A_3^0(q(k_1), \gamma^{\mathrm{id.}}(k_3), \bar{q}(k_3)) \, |M_2^0(\tilde{k}_1, \tilde{k}_2, p_i, p_j)|^2 \, J(\tilde{k}_1, \tilde{k}_2; z) \, \mathrm{d}\Phi_3$$

Jet function needs information about momentum fraction z of the photon within the quark-photon cluster Q_γ:

→ antenna phase space can not be fully integrated out

Integration over antenna phase space must remain differential in z:

$$\mathrm{d}\sigma_\gamma^T \propto -\int_0^1 \mathrm{d}z \underbrace{\left(\int \frac{\mathrm{d}\Phi_A}{\mathrm{d}z} A^0_{q\gamma\bar{q}} \right)}_{\mathscr{A}_3^0(z)} |M_2^0(\tilde{k}_1, \tilde{k}_2; p_i, p_j)|^2 \, J(\tilde{k}_1, \tilde{k}_2; z) \, \mathrm{d}\Phi_2$$

NNLO

- Subtraction of double unresolved limits (RR) and one-loop unresolved limits (RV)

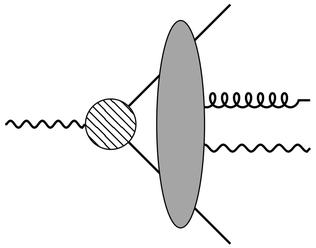

X_4^0

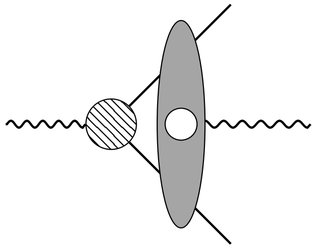

X_3^1

- Integration of fragmentation X_4^0 and X_3^1 while retaining information on momentum fraction z in one kinematic configuration (initial-final)

  → final-final configuration needed for identified hadrons
- Combining integrated antenna functions with counter-terms from fragmentation functions
- Inheritance of the momentum fraction z in consecutive unresolved limits

Integration of Fragmentation X_4^0

Necessary fragmentation antenna functions for photon production:

$\tilde{A}^0_{q,\gamma g q}$ subtracts $q \parallel g \parallel \gamma$ limit

$\tilde{E}^0_{q,q'\bar{q}'\gamma}$ subtracts the $q' \parallel \gamma \parallel \bar{q}'$ limit

Initial-final antenna phase space: $\mathrm{d}\Phi_A \propto \mathrm{d}\Phi_3(q(Q^2) + p_i \to k_1 + k_2 + \gamma(k_3))$

Additional δ-distribution in phase space integral fixes momentum fraction z:

$$\mathcal{X}_4^0(x,z) \propto \int \mathrm{d}^d k_1 \, \mathrm{d}^d k_2 \, \delta(k_1^2) \, \delta(k_2^2) \, \delta((p_i - q - k_1 - k_2)^2) \, \delta\left(z - \frac{s_{i3}}{s_{i1} + s_{i2} + s_{i3}}\right) X_4^0$$

For initial-final configuration: additional dependence on the initial-state momentum fraction x

Integration of Fragmentation X_4^0

Strategy:

Unitarity → replace δ-distributions by propagators

$$2\pi i\delta(k_1^2) = \frac{1}{k_1^2 + i\epsilon} - \frac{1}{k_1^2 - i\epsilon}$$

Phase space integral = cut through loop integral:

- Reduction of integrals using IBP-relations to 9 master integrals (MI)
- MI are calculated by solving differential equations in x and z
- Integration constants fixed by integrating over z and comparing to inclusive result

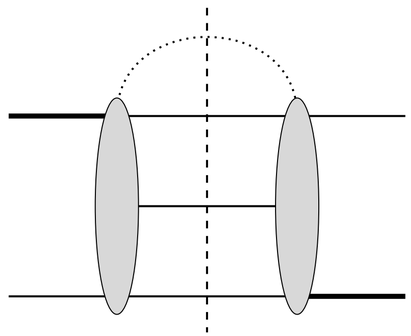

Integration of Fragmentation X_3^1

Antenna phase space in initial-final configuration:

$$\mathrm{d}\Phi_A \propto \mathrm{d}\Phi_2(q(Q^2) + p_i \to k_1 + \gamma(k_2))\,; \qquad z = \frac{s_{i2}}{s_{i2} + s_{i1}}$$

No actual integration has to be performed:

$$\mathcal{X}_3^1(x,z) = \frac{1}{C(\epsilon)} \int \frac{\mathrm{d}\Phi_2}{\mathrm{d}z} \frac{Q^2}{2\pi} X_3^1 = \frac{Q^2}{2} \frac{e^{\gamma_E \epsilon}}{\Gamma(1-\epsilon)} \left(Q^2\right)^{-\epsilon} \mathrm{J}^\gamma(x,z)\, X_3^1$$

However, X_3^1 has to be cast into a form suitable for an expansion in distributions in $1-x$ and z

Integration of Fragmentation X_3^1

X_3^1 can be expressed in terms of Box and Bubble MIs:

$$X_3^1(x,z) = \sum_{i=1}^{3} f_i(x,z)\,\mathrm{Box}_i(x,z) + \sum_{k=1}^{4} g_k(x,z)\,\mathrm{Bub}_k(x,z) + h(x,z)$$

$$\mathrm{Box}_i(x,z) \propto \sum_{j=1}^{3} \Big(r_{i,j}(x,z)\Big)^{-\epsilon}\, {}_2F_1(-\epsilon,-\epsilon;1-\epsilon;a_{i,j}(x,z))$$

Box-integrals: real-valued and well defined
in Euclidean region only

→ analytic continuation needed

Branch cuts ($a_{i,j}(x,z) = 1, \pm\infty$) within the physical region

→ distinguish different regions in the x-z-plane

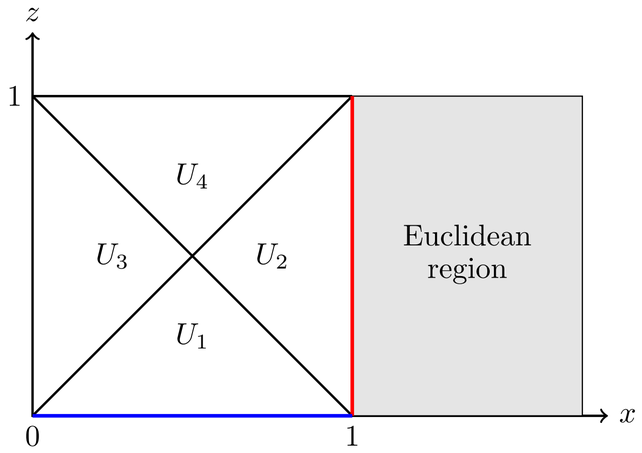

Inheritance of z

In consecutive unresolved limits a proper inheritance of z is required:

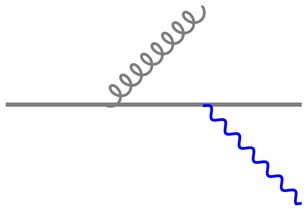

$\gamma \| q \xrightarrow[z_1]{}$

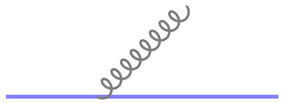

$g \| \tilde{q}_\gamma \xrightarrow[z_2]{}$

$$\underbrace{A_3^0(\bar{q}, \gamma^{\text{id.}}, q)}_{z_1} \underbrace{A_3^0(\bar{q}, g, \tilde{q}_\gamma^{\text{id.}})}_{z_2} \dots J(z = z_1 z_2)$$

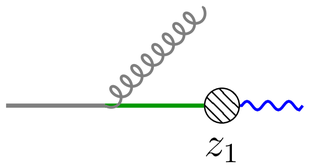

$q \| g \xrightarrow[z_2]{}$

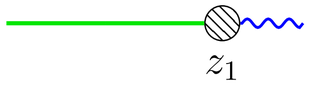

$$D_{q\to\gamma}(z_1) \underbrace{A_3^0(\bar{q}, g, q^{\text{id.}})}_{z_2} \dots J(z = z_1 z_2)$$

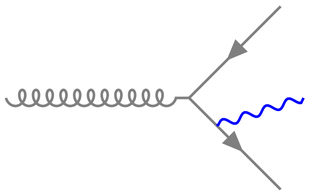

$\gamma \| q \xrightarrow[z_1]{}$

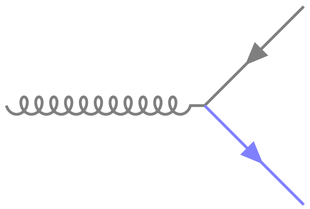

$\tilde{q}_\gamma \| \bar{q} \xrightarrow[z_2]{}$

$$\underbrace{A_3^0(\bar{q}, \gamma^{\text{id.}}, q)}_{z_1} \underbrace{E_3^0(q', \tilde{q}_\gamma^{\text{id.}}, \bar{q})}_{z_2} \dots J(z = z_1 z_2)$$

Subtraction Term

Subtraction term for subleading color matrix element $\tilde{\tilde{B}}_3^{\gamma,0}(\hat{q},\hat{g},g_1,g_2,q,\gamma)$

$$
\begin{aligned}
\mathrm{d}\sigma^{S,a}_{\mathrm{QCD}} &= +A^0_{3,q}(\hat{q},g_1,q)\,\tilde{B}^{G,0}_2(\bar{\hat{q}},\hat{g},g_2,\tilde{q}_{g_1},\gamma)\,J^{(3)}_1(\{\tilde{p}\}_3)\\
\mathrm{d}\sigma^{S,a}_{\gamma} &= +A^0_{3,q}(\hat{q},\gamma^{\mathrm{id.}},q)\,\tilde{\tilde{B}}^0_3(\bar{\hat{q}},\hat{g},g_1,g_2,\tilde{q}_{\gamma})\,J^{(3)}_1(\{\tilde{p}\}_3;z)\\
\mathrm{d}\sigma^{S,b}_{\gamma} &= +\tilde{A}^0_4(\hat{q},g_1,\gamma^{\mathrm{id.}},q)\,\tilde{B}^0_2(\bar{\hat{q}},\hat{g},g_2,\tilde{q}_{\gamma g_1})\,J^{(2)}_1(\{\tilde{p}\}_2;z)\\
&\quad -A^0_{3,q}(\hat{q},g_1,q)\,A^0_{3,q}(\bar{\hat{q}},\gamma^{\mathrm{id.}},\tilde{q}_{g_1})\,\tilde{B}^0_2(\bar{\bar{\hat{q}}},\hat{g},g_2,(\gamma\tilde{q}_{g_1}))\,J^{(2)}_1(\{\tilde{\tilde{p}}\}_2;z)\\
&\quad -A^0_{3,q}(\hat{q},\gamma^{\mathrm{id.}},q)\,A^0_{3,q}(\bar{\hat{q}},g_1,\tilde{q}^{\mathrm{id.}}_{\gamma})\,\tilde{B}^0_2(\bar{\bar{\hat{q}}},\hat{g},g_2,(g_1\tilde{q}_{\gamma}))\,J^{(2)}_1(\{\tilde{\tilde{p}}\}_2;z=z_1z_2)
\end{aligned}
$$

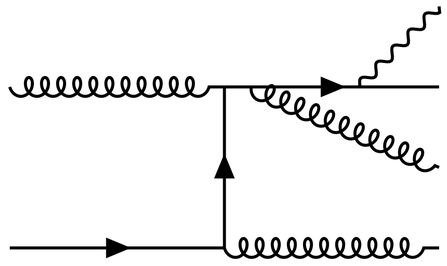

- $\mathrm{d}\sigma^{S,a}_{\mathrm{QCD}}$ and $\mathrm{d}\sigma^{S,a}_{\gamma}$ subtract the single unresolved limits of the matrix element
- $\mathrm{d}\sigma^{S,b}_{\gamma}$ subtract double unresolved limits of the matrix element

Full subtraction term: $\mathrm{d}\sigma^{S} = \mathrm{d}\sigma^{S,a}_{\mathrm{QCD}} + \mathrm{d}\sigma^{S,a}_{\gamma} + \mathrm{d}\sigma^{S,b}_{\mathrm{QCD}} + \mathrm{d}\sigma^{S,b}_{\gamma}$